

# Nuclear bound state of $\eta'(958)$ and partial restoration of chiral symmetry in the $\eta'$ mass

Daisuke Jido,<sup>1</sup> Hideko Nagahiro,<sup>2</sup> and Satoru Hirenzaki<sup>2</sup>

<sup>1</sup>*Yukawa Institute for Theoretical Physics, Kyoto University, Kyoto 606-8502, Japan*

<sup>2</sup>*Department of Physics, Nara Women's University, Nara 630-8506, Japan*

(Dated: December 6, 2018)

The in-medium mass of the  $\eta'$  meson is discussed in a context of partial restoration of chiral symmetry in nuclear medium. The  $\eta'$  mass is expected to be reduced by order of 100 MeV at the saturation density. The reduction is a consequence of the suppression of the anomaly effect on the  $\eta'$  mass induced by partial restoration of chiral symmetry. This strong attraction in  $\eta'$  nuclear systems does not accompany large absorption of  $\eta'$  into nuclear matter. This leads to the possibility of so narrow bound states of the  $\eta'$  meson in nuclei to be seen in hadronic reactions with light nuclear targets.

PACS numbers: 21.85.+d, 25.80.Hp, 14.40.Be

The  $U_A(1)$  problem [1] has attracted continuous attention for a long time as a fundamental question on the low-energy spectrum and dynamics of the pseudoscalar mesons in QCD. Since quantum gluon dynamics explicitly breaks the  $U_A(1)$  symmetry, the  $\eta'$  meson is not necessarily a Nambu-Goldstone boson associated with spontaneous chiral symmetry breaking. Thus, the peculiarly large mass of the  $\eta'$  meson is a consequence of the quantum anomaly [2] inducing the non-trivial vacuum structure of QCD [3, 4]. It is also known that the  $\eta'$  spectrum strongly depends on the breaking pattern of chiral symmetry [5].

The study of dynamical chiral symmetry breaking and its partial restoration at finite density systems is one of the important subjects of contemporary hadron-nuclear physics. Recent experimental observations of pionic atoms [6], especially deeply bound states in Sn isotopes [7], and low-energy pion-nucleus scattering [8, 9] have figured out with helps of theoretical analyses [10, 11] whether the partial restoration does take place in nuclei with order of 30% reduction of the quark condensate. It goes a step further to the stage of precise determination of the density dependence of the quark condensate both in theory and experiment [12, 13], and systematic studies of the partial restoration appearing in other meson-nuclear systems. As shown later, since the chiral symmetry breaking plays an important role also for the  $\eta'$  mass generation, one expects strong mass reduction due to the partial restoration.

One of the efficient ways to observe in-medium modification of the meson properties is spectroscopy of meson-nucleus bound systems like deeply bound pionic atoms. The main advantage to observe the meson-nucleus bound system is that it is guaranteed that the meson inhabits the nucleus and it is unnecessary to remove in-vacuum contributions from the spectrum. So far several meson nuclear bound states have been proposed [14–17] and experimental attempts of the bound state observation have been performed [18, 19]. Nevertheless, there are difficulties to observe clear signals for the mesonic bound states, because the bound states have large absorption widths due to strong interactions, such as conversion into lighter

mesons and two nucleon absorptions [20–22].

The purposes of the present paper are twofold: Firstly, we shed light upon the  $\eta'$  meson mass in nuclear matter in the context of partial restoration of chiral symmetry, pointing out that the  $U_A(1)$  anomaly effects causes the  $\eta'$ - $\eta$  mass difference necessarily through the chiral symmetry breaking. This fact leads to a relatively large mass reduction and weak absorption for  $\eta'$  in nuclear matter. Thus, we expect that possible nuclear bound states of the  $\eta'$  meson have narrower widths than their level spacings. Secondly, we discuss experimental visibility of the  $\eta'$  bound states by showing typical formation spectra of the  $\eta'$  mesonic nuclei using a simple optical potential of  $\eta'$  in nuclei which incorporates our theoretical consideration.

Theoretical investigations of the  $\eta'$  meson in finite energy density hadronic matter have been performed since long ago [23–25], but the present status of the study of  $\eta'$ -nucleus interaction is still exploratory due to lack of experimental information and our knowledge of the fate of the  $U_A(1)$  anomaly in nuclei is rather short. The reduction of the  $\eta'$  mass in finite density systems has been suggested in several theoretical approaches. For instance, it has been pointed out that the  $\eta'$  mass is reduced at finite density due to rapid decrease of the instanton effects caused by strong suppression of the tunneling between different topological vacua [25]. In Nambu–Jona-Lasinio model calculations, 150 MeV mass reduction at the saturation density was suggested by using no density dependent determinant interaction [26], while with the density dependence 250 MeV reduction was reported in Ref. [27]. Experimentally, it has been reported that a strong reduction of the  $\eta'$  mass, at least 200 MeV, is necessary to explain the two-pion correlation in Au + Au collisions at RHIC [28, 29]. On the other hand, analyses of the low-energy  $\eta'$  production experiment with  $pp$  collisions have suggested relatively smaller  $\eta'$ -proton scattering lengths,  $|\text{Re } a_{\eta'p}| < 0.8 \text{ fm}$  [30] and  $|a_{\eta'p}| \sim 0.1 \text{ fm}$  [31], which correspond to from several to tens MeV mass reduction at the nuclear saturation density if it is estimated by the linear density approximation.

It is notable that the transparency ratios of the  $\eta'$

meson in nuclei were also observed in TAPS and has suggested the absorption width of the  $\eta'$  meson at the saturation density is as small as around 30 MeV [32]. In Ref. [33], it is reported that the  $\eta'NN$  three point vertex should be suppressed according to an extended Goldberger-Treiman relation. Thus, the  $\eta'$  absorption into nuclear matter is possibly smaller.

The basic idea of the present work is that one should distinguish between the anomaly operator itself and anomaly effects which are represented by matrix elements of the anomaly operator. The  $U_A(1)$  quantum anomaly appears in the divergence of the flavor singlet axial vector current:

$$\partial^\mu A_\mu^{(0)} = 2i(m_u \bar{u}\gamma_5 u + m_d \bar{d}\gamma_5 d + m_s \bar{s}\gamma_5 s) + \frac{3\alpha_s}{8\pi} F\tilde{F}. \quad (1)$$

The terms in the parentheses are the PCAC contributions and vanish in the chiral limit, while the last term in the right hand side is the  $U_A(1)$  anomaly term coming from gluon dynamics. Due to the last term the axial current does not conserve even in the chiral limit. Since Eq. (1) is an operator relation, in order that the anomaly affects the  $\eta'$  mass, the operator  $F\tilde{F}$  should couple to the  $\eta'$  state. This implies that it may happen that, even though the anomaly term is present in Eq. (1) and breaks the  $U_A(1)$  symmetry, the anomaly term does not couple to the  $\eta'$  state and the  $\eta'$  mass is not affected by the anomaly.

We see that this is the case when the  $SU(3)_L \otimes SU(3)_R$  chiral symmetry is restored in the following symmetry argument (see also a dynamical argument given in Ref. [5]). For simplicity we consider the three flavor chiral limit. The mass spectra of the flavor singlet and octet pseudoscalar mesons is described by the correlation functions  $\langle 0|T\phi_5^a(x)\phi_5^{b\dagger}(0)|0\rangle$  with the pseudoscalar field  $\phi_5^a \equiv \bar{q}i\gamma_5\lambda^a q$  ( $a = 0, 1, \dots, 8$ ) with the quark field  $q$  and the Gell-Mann matrix  $\lambda^a$  for the  $SU(3)$  flavor. Because both flavor singlet and octet pseudoscalar fields belong to the same  $(\mathbf{3}, \mathbf{3}) \oplus (\mathbf{3}, \mathbf{3})$  chiral multiplet of the  $SU(3)_L \otimes SU(3)_R$  group, when the  $SU(3)_L \otimes SU(3)_R$  chiral symmetry is manifest, the flavor singlet and octet spectra should degenerate, no matter how the  $U_A(1)$  anomaly depends on the density. Therefore, this symmetry argument concludes that the  $\eta$  and  $\eta'$  mass splitting can take place only with (dynamical and/or explicit) chiral symmetry breaking, meaning that the  $U_A(1)$  anomaly effect does push the  $\eta'$  mass up necessarily with the chiral symmetry breaking.

In other words, the chiral singlet gluonic operator, which makes the  $\eta'$  mass lift up, cannot couple to the chiral pseudoscalar state without breaking chiral symmetry. In the large- $N_c$  argument of Refs. [2, 34], the  $\eta'$  mass can be obtained by the consistency condition that there should be cancellation between the flavor-singlet pseudoscalar pole and the gauge-dependent massless ghost in the correlation function of the topological charge density  $F\tilde{F}$  in the soft limit. Performing the topological expan-

sion of the quark loop, one has at the chiral limit [2, 35]

$$m_{\eta'}^2 = \frac{N_c c_{\eta'}^2}{U_0(0)} \quad (2)$$

with the matrix element of  $F\tilde{F}$  to create the  $\eta'$  meson

$$\sqrt{N_c} c_{\eta'} = \langle 0|F\tilde{F}|\eta'\rangle, \quad (3)$$

the number of color  $N_c$  and  $U_0(0)$  being the value of the topological charge density correlator at the soft limit obtained without the quark loop, namely in the pure Yang-Mills theory. Since chiral symmetry should be broken for the nonzero value of the matrix element  $c_{\eta'}$ , the mass relation (2) shows that, when chiral symmetry is being restored and the matrix element  $c_{\eta'}$  is getting reduced, the mass of the flavor singlet  $\eta'$  should be going down, even if  $F\tilde{F}$  appears in the divergence of the axial current.

In this way the mass splitting of the  $\eta$ - $\eta'$  mesons is a consequence of the interplay of the  $U_A(1)$  anomaly effect and the chiral symmetry breaking. Assuming 30% reduction of the quark condensate in nuclear medium and that the mass difference of  $\eta$  and  $\eta'$  comes from the quark condensate linearly, one could expect an order of 150 MeV attraction for the  $\eta'$  meson coming from partial restoration of chiral symmetry in nuclear medium. This attraction is much stronger than, for instance, that for  $\eta$  estimated in a chiral unitary model, which is as order of 50 MeV at the saturation density [36].

The present mechanism of the  $\eta'$  mass reduction in finite density has another unique feature. In usual cases, attractive interactions of in-medium mesons induced by hadronic many-body effects unavoidably accompany comparably large absorptions. This can be perceived from the fact that the dispersion relation for the meson self-energy connects its real and imaginary parts as a consequence of the  $s$ -channel unitarity. This leads to the consequence that possible bound states have a comparable absorption width with the binding energy. For the attraction induced by gluon dynamics, like the present case, although some many-body effects introduce an absorptive potential for the  $\eta'$  meson in medium, the mass reduction mechanism does not involve hadronic intermediate states and, thus, the attraction dose not accompany an additional imaginary part. Furthermore, in the present case, since the suppression of the  $U_A(1)$  anomaly effect induces the attractive interaction, the influence acts selectively on the  $\eta'$  meson and, thus, it does not induce inelastic transitions of the  $\eta'$  meson into lighter mesons in nuclear medium. Consequently the  $\eta'$  absorption in nuclear matter can be small, which is consistent with the experimental finding [32].

As seen in the above observation, the  $\eta'$  mass is to be largely reduced in nuclear matter due to the suppression of the anomaly effect and simultaneously the absorption into nuclear matter can be small. Certainly with this attraction some bound states for  $\eta'$  in nuclei are formed. The question is whether the bound states are enough separated each other with so narrow widths as to be observed

in formation experiments. To observe clear signals of the bound states in formation experiments, first of all, it is important to choose appropriate nuclear targets of the reactions. Here we suggest nuclei with  $A \sim 10$ , such as  $^{12}\text{C}$ , as the target, since these nuclei may provide us with finite density nuclear systems rather than systems with few-body characters. As for heavier nuclei, we have several shell states for nucleons, which make the formation spectrum complicated for the analyses as we will mention later.

Let us sketch  $\eta'$  bound state structure in a nucleus expected by the present argument and show formation spectra of the  $\eta'$  mesonic nucleus in the  $^{12}\text{C}(\pi^+, p)^{11}\text{C} \otimes \eta'$  reaction. We exploit a simple phenomenological optical potential of the  $\eta'$  meson in nuclei as

$$V_{\eta'}(r) = V_0 \frac{\rho(r)}{\rho_0}, \quad (4)$$

with the Woods-Saxon type density distribution  $\rho(r)$  for nucleus and the saturation density  $\rho_0 = 0.17 \text{ fm}^{-3}$ . The depth of the attractive potential is a order of 100 MeV at the normal nuclear density as discussed above and the absorption width is expected to be less than 40 MeV [32] which corresponds to the 20 MeV imaginary part of the optical potential.

In Fig. 1, we show the bound state spectra of the  $\eta'$  bound states,  $B_\eta \equiv E_{KG} - m_{\eta'}$ , in  $^{11}\text{C}$ , which is the residual nucleus in the  $^{12}\text{C}(\pi^+, p)$  reaction. The Klein-Gordon energy  $E_{KG}$  is obtained as a complex value by solving the Klein-Gordon equation with the  $\eta'$  optical potential in the form of Eq. (4) assuming the depths to be  $\text{Re}V_0 = -100, -150, -200 \text{ MeV}$  with  $\text{Im}V_0 = -20 \text{ MeV}$ . As seen in the figure, thanks to the strong attraction, there are several bound states in such a small nucleus, and, in addition, due to the small absorption these bound states are well separated. In contrast, as shown in Fig. 1, optical potentials having a comparable imaginary part with the real part, such as  $\text{Re}V_0 = -100 \text{ MeV}$  and  $\text{Im}V_0 = -50 \text{ MeV}$ , provide bound states which have larger widths than the binding energies. In this case it will be hard to observe these bound states as clear peaks in the formation spectra. For the detailed spectral structure of the bound states, the nuclear polarization will be important for the strongly interacting meson [37]. We have checked, by assuming possible polarization of the core nucleus evaluated in a kaonic system with the 160 MeV binding energy [37], that the core polarization effect shifts the bound state levels downwards but the bound states are so separated to be seen as isolated peaks.

In order to see the visibility of the peak structure of the bound state spectrum in experiments, we calculate the formation spectra of the  $\eta'$  mesonic nuclei. We use the  $^{12}\text{C}(\pi^+, p)$  reaction with the 1.8 GeV/c incident  $\pi^+$  beam to produce the  $\eta'$ -nucleus system. Since the  $\eta'$  production in this reaction is exothermic, one cannot achieve the recoilless condition for the  $\eta'$  in nuclei. One observes the spectrum of the  $\eta'$ -nucleus system by detecting the emitted proton at the forward direction in order to reduce

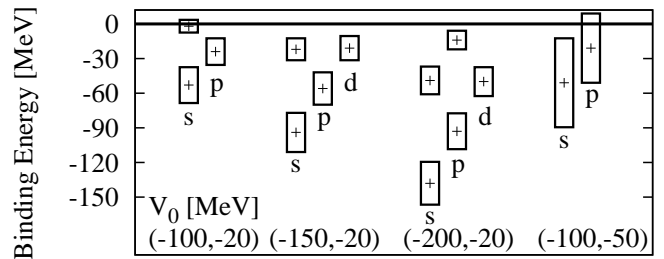


FIG. 1. Bound state spectra of the  $\eta'$  meson in  $^{11}\text{C}$  in units of MeV. Cross denotes the binding energy and the band indicates the width of the bound state. The letters, s, p, d label the angular momentum states. The optical potential of the  $\eta'$  meson in the nucleus is assumed in the form of Eq. (4) with the potential depths at the normal nuclear density  $\text{Re}V_0 = -100, -150$  and  $-200 \text{ MeV}$  with a fixed imaginary potential  $\text{Im}V_0 = -20 \text{ MeV}$ . We also show a result with the larger imaginary potential  $\text{Im}V_0 = -50 \text{ MeV}$  with  $\text{Re}V_0 = -100 \text{ MeV}$ .

the momentum transfer.

The formation spectrum is calculated in the approach developed in Refs. [22, 38–41]. The calculated spectrum is scaled by the forward differential cross section of the elementary  $\pi^+ n \rightarrow \eta' p$  process, which is estimated to be  $100 \mu\text{b/sr}$  in the laboratory frame from the total cross section  $\sigma \sim 100 \mu\text{b}$  [42] under the assumption of isotropic angular dependence in the center of mass frame. We calculate the formation spectra separately in the subcomponents of the  $\eta'$ -mesonic nuclei labeled by  $(n\ell_j)_n^{-1} \otimes \ell_{\eta'}$  that indicates the formation of an  $\eta'$  meson in the  $\ell_{\eta'}$  orbit with a neutron-hole in the  $\ell$  orbit with the total spin  $j$  and the principal quantum number  $n$  in the daughter nucleus. The calculated spectra are shown as functions of  $E_{\text{ex}} - E_0$  where  $E_0$  is the  $\eta'$  production threshold with the ground state daughter nucleus and the excitation energy  $E_{\text{ex}}$  is defined by  $E_{\text{ex}} \equiv m_{\eta'} - B_{\eta'} + [S_n(j_n) - S_n(0p_{3/2})]$  with  $S_n(j_n)$  being the neutron separation energy from the neutron single-particle level  $j_n$  to take into account the difference of the separation energy  $S_n(j_n) - S_n(0p_{3/2}) = 18 \text{ MeV}$  for the subcomponents accompanied by the  $(0s_{1/2})_n^{-1}$  hole-state.

In Fig. 2, we show the calculated  $^{12}\text{C}(\pi^+, p)^{11}\text{C} \otimes \eta'$  cross sections with three different potential parameters. (See the figure caption.) In the figure, the vertical line at  $E_{\text{ex}} - E_0 = 0$  indicates the  $\eta'$  production threshold in vacuum. In the case of no attractive potential, there is no structure in the  $\eta'$ -binding region but some bump in the quasi-free region. Taking this case as a reference, we discuss the structure of the formation spectra with the attractive potentials. In each plot, the subcomponents with the  $(0s_{1/2})_n^{-1}$  hole-state give less contributions, because there are only half the neutrons in the  $s_{1/2}$  state of the  $p_{3/2}$  neutrons in the parent nucleus. Finding so prominent peaks in the  $\eta'$ -binding region as to be possibly observed in future experiments, we conclude that with an order of 100 MeV mass reduction and a 40 MeV absorp-

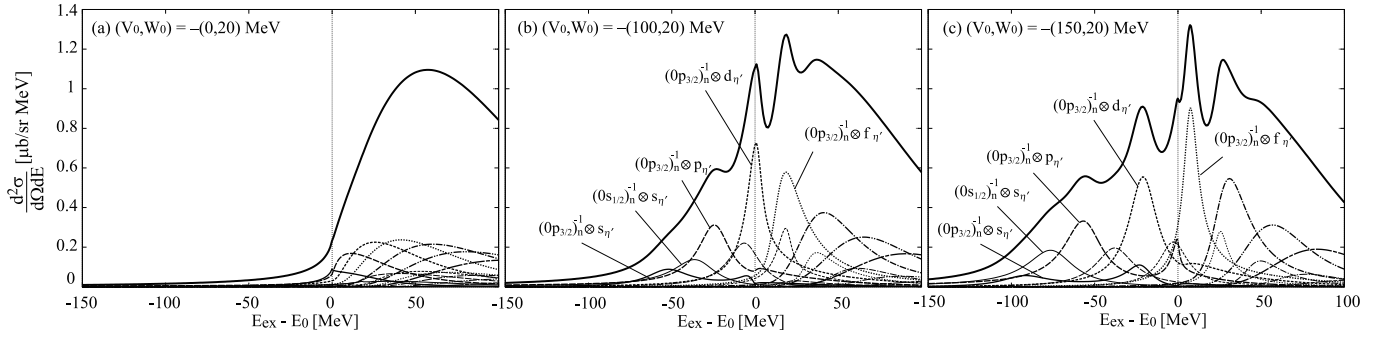


FIG. 2. Calculated spectra of the  $^{12}\text{C}(\pi^+, p)^{11}\text{C}\otimes\eta'$  at  $p_\pi = 1.8$  GeV/c as functions of the excitation energy  $E_{\text{ex}}$  with (a)  $V_0 = -(0 + 20i)$  MeV, (b)  $V_0 = -(100 + 20i)$  MeV and (c)  $V_0 = -(150 + 20i)$  MeV. The thick solid lines show the total spectra, and the dominant subcomponents are labeled by the neutron-hole state  $(n\ell_j)_n^{-1}$  and the  $\eta'$  state  $\ell_{\eta'}$ .

tion width at the saturation density we have a chance to observe the  $\eta'$ -nucleus bound states in the  $^{12}\text{C}(\pi^+, p)$  reaction. We see also clear peaks around the  $\eta'$  production threshold, for instance  $(0p_{3/2})_n^{-1} \otimes d_{\eta'}$  in plot (b) and  $(0p_{3/2})_n^{-1} \otimes f_{\eta'}$  in plot (c). They are not signals of the bound states, because no bound states exist in the  $d$  and  $f$  states for the case (b) and (c), respectively, as shown in Fig. 1. Nevertheless, these are remnants of the bound states which could be formed if the attraction would be stronger. Therefore, such peak structure also can be signals of the strong attractive potential.

Similarly to hypernucleus production spectra in the  $(\pi^+, K^+)$  reaction, in the obtained spectra shown in Fig. 2 many subcomponents with different quantum numbers give certain contributions because of the finite momentum transfer (200 MeV/c) in the present reaction. Thus, to identify the quantum number of each peak, precise measurements and theoretical analyses are necessary. Nevertheless, observing peak structure is the important first step to perform detailed spectroscopy of the  $\eta'$  bound states. As seen in Refs. [17, 27, 43], the structure of the formation spectra is not so dependent on the formation reaction of the  $\eta'$  mesonic nuclei.

The experimental feasibility for the observation of the peak structure highly depends on the level spacing of the bound states and their widths. Since  $\eta'$  is in the Wood-Saxon type potential induced by the nuclear density, the level spacing of the  $\eta'$  bound states in a nucleus with mass number  $A$  is characterized as  $\hbar\omega \sim 40A^{-1/3}$  MeV similarly to the major shell spacing for nuclei. For observation of clear peak structure, the level spacing should be larger than the level width  $\Gamma \sim -2\text{Im}V$ . For the  $^{12}\text{C}$  target

case, the upper limit would be  $\Gamma = -2\text{Im}V \sim 50$  MeV, which is larger than  $\Gamma = 25\text{--}30$  MeV extracted from the transparency ratio at  $p = 0.95$  GeV/c in Ref. [32]. For larger  $A$ , even though the formation cross section can be larger, the peak structure gets less prominent because of the following reason. The bound state spectrum is determined by convolutions of the nucleon hole and  $\eta'$  bound wavefunction. For larger  $A$ , there are more levels of the hole state and the level spacing of the  $\eta'$  bound states are smaller. Consequently the peaks coming from many possible combinations get overlapped and the peak structure is smeared out. Thus, nuclei with  $A \sim 10$  to 20 are good candidates of the target for the formation experiments.

In conclusion, we point out that partial restoration of chiral symmetry in a nuclear medium induces suppression of the  $U_A(1)$  anomaly *effect* to the  $\eta'$  mass. Consequently, we expect a large mass reduction of the  $\eta'$  meson in nuclear matter with relatively smaller absorption. The mass reduction could be observed as  $\eta'$ -nucleus bound states in the formation reactions. The interplay between the chiral symmetry restoration and the  $U_A(1)$  anomaly effect can be a clue to understand the  $\eta'$  mass generation mechanism. Therefore, experimental observations of the deeply  $\eta'$ -nucleus bound states, or even confirmation of nonexistence of such deeply bound states, is important to understand the  $U_A(1)$  anomaly effects on hadrons.

*Acknowledgement.* The authors would like to thank Dr. K. Itahashi, Dr. H. Fujioka and Prof. W. Weise for useful discussion. This work was partially supported by the Grants-in-Aid for Scientific Research (No. 22740161, No. 20540273, and No. 22105510). This work was done in part under the Yukawa International Program for Quark-hadron Sciences (YIPQS).

[1] S. Weinberg, Phys. Rev. **D11**, 3583 (1975).  
[2] E. Witten, Nucl. Phys. **B156**, 269 (1979).  
[3] G. 't Hooft, Phys. Rev. **D14**, 3432 (1976).  
[4] G. 't Hooft, Phys. Rev. Lett. **37**, 8 (1976).  
[5] S. H. Lee and T. Hatsuda, Phys. Rev. **D54**, 1871 (1996).

[6] E. Friedman and A. Gal, Nucl. Phys. **A724**, 143 (2003).  
[7] K. Suzuki *et al.*, Phys. Rev. Lett. **92**, 072302 (2004).  
[8] E. Friedman *et al.*, Phys. Rev. Lett. **93**, 122302 (2004).  
[9] E. Friedman *et al.*, Phys. Rev. **C72**, 034609 (2005).  
[10] E. E. Kolomeitsev, N. Kaiser, and W. Weise, Phys. Rev.



- Lett. **90**, 092501 (2003).
- [11] D. Jido, T. Hatsuda, and T. Kunihiro, Phys. Lett. **B670**, 109 (2008).
  - [12] N. Kaiser, P. de Homont, and W. Weise, Phys. Rev. **C77**, 025204 (2008).
  - [13] N. Ikeno *et al.*, Prog. Theor. Phys. **126**, 483 (2011).
  - [14] Q. Haider and L. C. Liu, Phys. Lett. **B172**, 257 (1986).
  - [15] R. S. Hayano, S. Hirenzaki, and A. Gillitzer, Eur. Phys. J. **A6**, 99 (1999).
  - [16] T. Kishimoto, Phys. Rev. Lett. **83**, 4701 (1999).
  - [17] H. Nagahiro and S. Hirenzaki, Phys. Rev. Lett. **94**, 232503 (2005).
  - [18] R. E. Chrien *et al.*, Phys. Rev. Lett. **60**, 2595 (1988).
  - [19] T. Kishimoto *et al.*, Prog. Theor. Phys. Suppl. **149**, 264 (2003).
  - [20] M. Kohno and H. Tanabe, Phys. Lett. **B231**, 219 (1989).
  - [21] J. Yamagata, H. Nagahiro, and S. Hirenzaki, Phys. Rev. **C76**, 014604 (2006).
  - [22] H. Nagahiro, D. Jido, and S. Hirenzaki, Phys. Rev. **C80**, 025205 (2009).
  - [23] R. D. Pisarski and F. Wilczek, Phys. Rev. **D29**, 338 (1984).
  - [24] T. Kunihiro, Phys. Lett. **B219**, 363 (1989).
  - [25] J. I. Kapusta, D. Kharzeev, and L. D. McLerran, Phys. Rev. **D53**, 5028 (1996).
  - [26] P. Costa, M. C. Ruivo, and Y. L. Kalinovsky, Phys. Lett. **B560**, 171 (2003).
  - [27] H. Nagahiro, M. Takizawa, and S. Hirenzaki, Phys. Rev. **C74**, 045203 (2006).
  - [28] T. Csörgő, R. Vértési, and J. Sziklai, Phys. Rev. Lett. **105**, 182301 (2010).
  - [29] R. Vértési, T. Csörgő, and J. Sziklai, Phys. Rev. C **83**, 054903 (2011).
  - [30] P. Moskal *et al.*, Phys. Lett. **B474**, 416 (2000).
  - [31] P. Moskal *et al.*, Phys. Lett. **B482**, 356 (2000).
  - [32] M. Nanova, (2010), talk in Baryons10, Dec 7-12, 2010, Osaka Univ., Osaka, Japan.
  - [33] G. Veneziano, Mod. Phys. Lett. **A4**, 1605 (1989).
  - [34] G. Veneziano, Nucl. Phys. **B159**, 213 (1979).
  - [35] G. A. Christos, Phys. Rept. **116**, 251 (1984).
  - [36] T. Inoue and E. Oset, Nucl. Phys. **A710**, 354 (2002).
  - [37] J. Mares, E. Friedman, and A. Gal, Nucl. Phys. **A770**, 84 (2006).
  - [38] D. Jido, H. Nagahiro, and S. Hirenzaki, Phys. Rev. **C66**, 045202 (2002).
  - [39] H. Nagahiro, D. Jido, and S. Hirenzaki, Phys. Rev. **C68**, 035205 (2003).
  - [40] H. Nagahiro, D. Jido, and S. Hirenzaki, Nucl. Phys. **A761**, 92 (2005).
  - [41] D. Jido, E. E. Kolomeitsev, H. Nagahiro, and S. Hirenzaki, Nucl. Phys. **A811**, 158 (2008).
  - [42] R. Rader *et al.*, Phys. Rev. **D6**, 3059 (1972).
  - [43] H. Nagahiro, Prog. Theor. Phys. Suppl. **186**, 316 (2010).